

Supporting information for:

Tipping the balance between concerted versus sequential proton-coupled electron transfer

Joshua S. Kretchmer and Thomas F. Miller III*

*Department of Chemistry and Chemical Engineering, California Institute of Technology, Pasadena,
California 91125*

E-mail: tfm@caltech.edu

Contents

1	Ring polymer molecular dynamics	S1
2	Systems	S5
2.1	Atomistic Representation for PCET	S5
2.2	System-bath Representation for PCET	S10
3	Calculation details	S13
3.1	Atomistic representation	S13
3.1.1	Collective variables	S15
3.1.2	RPMD rate calculations for concerted PCET	S18
3.1.3	RPMD rate calculations for ET prior to PT	S20
3.1.4	1D FE profile for PT prior to ET	S21

*To whom correspondence should be addressed

3.1.5	Two-dimensional FE profiles	S22
3.1.6	Solvent reorganization energy for concerted PCET	S23
3.1.7	Solvent reorganization energy for ET prior to PT	S24
3.1.8	Solvent reorganization energy for symmetric ET	S25
3.1.9	RPMD transition path ensemble	S26
3.2	System-bath representation	S26
3.2.1	Collective Variables	S27
3.2.2	RPMD rate calculations for concerted PCET	S27
3.2.3	RPMD rate calculations for ET prior to PT	S29
4	Auxiliary restraining potentials	S30
4.1	Auxiliary restraining potential for concerted PCET in the atomistic models .	S30
4.2	Auxiliary restraining potential for ET prior to PT in the atomistic models . .	S31
4.3	Auxiliary restraining potential for concerted PCET in the system-bath models	S32
4.4	Auxiliary restraining potential for ET prior to PT in the system-bath models	S33

1 Ring polymer molecular dynamics

The RPMD equations of motion for a quantized electron, a quantized proton and N classical particles, including a mixed-bead-number path-integral representation, are presented as Eqs. 1-3 in the main text and re-stated below for clarity,^{S1-S4}

$$\begin{aligned}
\dot{\mathbf{v}}_{\mathbf{e}}^{(\alpha)} &= \omega_{n_e}^2 \left(\mathbf{q}_{\mathbf{e}}^{(\alpha+1)} + \mathbf{q}_{\mathbf{e}}^{(\alpha-1)} - 2\mathbf{q}_{\mathbf{e}}^{(\alpha)} \right) \\
&- \frac{1}{m_e} \nabla_{\mathbf{q}_{\mathbf{e}}^{(\alpha)}} U \left(\mathbf{q}_{\mathbf{e}}^{(\alpha)}, \mathbf{q}_{\mathbf{p}}^{((\alpha-k)\frac{1}{n_{ep}}+1)}, \mathbf{Q} \right),
\end{aligned} \tag{S.1}$$

$$\begin{aligned}
\dot{\mathbf{v}}_{\mathbf{p}}^{(\gamma)} &= \omega_{n_p}^2 \left(\mathbf{q}_{\mathbf{p}}^{(\gamma+1)} + \mathbf{q}_{\mathbf{p}}^{(\gamma-1)} - 2\mathbf{q}_{\mathbf{p}}^{(\gamma)} \right) \\
&- \frac{1}{m_p} \sum_{l=1}^{n_{ep}} \nabla_{\mathbf{q}_{\mathbf{p}}^{(\gamma)}} U \left(\mathbf{q}_{\mathbf{e}}^{((\gamma-1)n_{ep}+l)}, \mathbf{q}_{\mathbf{p}}^{(\gamma)}, \mathbf{Q} \right),
\end{aligned} \tag{S.2}$$

and

$$\dot{\mathbf{V}}_j = -\frac{1}{n_e M_j} \sum_{\gamma=1}^{n_p} \sum_{l=1}^{n_{ep}} \nabla_{\mathbf{Q}_j} U \left(\mathbf{q}_e^{((\gamma-1)n_{ep}+l)}, \mathbf{q}_p^{(\gamma)}, \mathbf{Q} \right), \quad (\text{S.3})$$

where n_e is the number of imaginary-time ring-polymer beads for the transferring electron, m_e is the physical mass for the electron, and $\mathbf{q}_e^{(\alpha)}$ and $\mathbf{v}_e^{(\alpha)}$ are the respective position and velocity vectors for the α th ring-polymer bead of the electron; the corresponding quantities for the transferring proton are indicated using subscript “p”. In Eqs. (S.1)-(S.3), it is assumed that $n_{ep} = n_e/n_p$ is an integer number, and

$$k = \alpha - n_{ep} \left\lfloor \frac{\alpha - 1}{n_{ep}} \right\rfloor, \quad (\text{S.4})$$

where $\lfloor \dots \rfloor$ denotes the floor function. The periodic constraint of the ring-polymer is satisfied via $\mathbf{q}_e^{(0)} = \mathbf{q}_e^{(n_e)}$ and $\mathbf{q}_p^{(0)} = \mathbf{q}_p^{(n_p)}$, and the intra-bead harmonic frequencies are $\omega_{n_e} = n_e/(\beta\hbar)$ and $\omega_{n_p} = n_p/(\beta\hbar)$, where $\beta = 1/k_B T$ is the inverse temperature. The position, velocity, and mass for the j th classical degree of freedom are given by \mathbf{Q}_j , \mathbf{V}_j , and M_j , respectively, and $\mathbf{Q} = \{\mathbf{Q}_1, \dots, \mathbf{Q}_N\}$. Lastly, the potential energy function of the system is given by $U(\mathbf{q}_e, \mathbf{q}_p, \mathbf{Q})$.

Analogous to the classical thermal rate constant,^{S5-S7} the RPMD thermal rate constant can be expressed as^{S8,S9}

$$k_{\text{RPMD}} = \lim_{t \rightarrow \infty} \kappa(t) k_{\text{TST}}, \quad (\text{S.5})$$

where k_{TST} is the transition state theory (TST) estimate for the rate associated with the dividing surface $\zeta(\mathbf{r}) = \zeta^\ddagger$, $\zeta(\mathbf{r})$ is a collective variable that distinguishes between the reactant and product basins of stability, and $\kappa(t)$ is the time-dependent transmission coefficient that accounts for recrossing of trajectories through the dividing surface. We have introduced $\mathbf{r} = \{\mathbf{q}_e^{(1)}, \dots, \mathbf{q}_e^{(n_e)}, \mathbf{q}_p^{(1)}, \dots, \mathbf{q}_p^{(n_p)}, \mathbf{Q}_1, \dots, \mathbf{Q}_N\}$ to denote the position vector for the full system in the ring-polymer representation. As is the case for both exact classical and exact quantum dynamics, the RPMD method yields reaction rates and mechanisms

that are independent of the choice of dividing surface.^{S8–S10}

The TST rate in Eq. (S.5) is calculated using^{S11–S14}

$$k_{\text{TST}} = (2\pi\beta)^{-1/2} \langle g_{\tilde{\zeta}} \rangle_{\text{c}} \frac{e^{-\beta\Delta F(\tilde{\zeta}^\ddagger)}}{\int_{-\infty}^{\tilde{\zeta}^\ddagger} d\tilde{\zeta} e^{-\beta\Delta F(\tilde{\zeta})}}, \quad (\text{S.6})$$

where $F(\tilde{\zeta})$ is the free energy (FE) along $\tilde{\zeta}$,

$$e^{-\beta\Delta F(\tilde{\zeta})} = \frac{\langle \delta(\tilde{\zeta}(\mathbf{r}) - \tilde{\zeta}) \rangle}{\langle \delta(\tilde{\zeta}(\mathbf{r}) - \tilde{\zeta}_r) \rangle}, \quad (\text{S.7})$$

$\tilde{\zeta}_r$ is a reference point in the reactant basin, and^{S13,S15–S17}

$$g_{\tilde{\zeta}}(\mathbf{r}) = \left[\sum_{i=1}^d \frac{1}{m_i} \left(\frac{\partial \tilde{\zeta}(\mathbf{r})}{\partial r_i} \right)^2 \right]^{1/2}. \quad (\text{S.8})$$

Here, r_i is an element of the position vector \mathbf{r} , m_i is the corresponding physical mass, and d is the length of vector \mathbf{r} . The equilibrium ensemble average is denoted

$$\langle \dots \rangle = \frac{\int d\mathbf{r} \int d\mathbf{v} e^{-\beta H(\mathbf{r}, \mathbf{v})} (\dots)}{\int d\mathbf{r} \int d\mathbf{v} e^{-\beta H(\mathbf{r}, \mathbf{v})}}, \quad (\text{S.9})$$

and the average over the ensemble constrained to the dividing surface is denoted

$$\langle \dots \rangle_{\text{c}} = \frac{\int d\mathbf{r} \int d\mathbf{v} e^{-\beta H(\mathbf{r}, \mathbf{v})} (\dots) \delta(\tilde{\zeta}(\mathbf{r}) - \tilde{\zeta}^\ddagger)}{\int d\mathbf{r} \int d\mathbf{v} e^{-\beta H(\mathbf{r}, \mathbf{v})} \delta(\tilde{\zeta}(\mathbf{r}) - \tilde{\zeta}^\ddagger)}, \quad (\text{S.10})$$

where

$$\begin{aligned} H(\mathbf{r}, \mathbf{v}) &= \sum_{j=1}^N \frac{1}{2} M_j \mathbf{V}_j^2 + \sum_{\alpha=1}^{n_e} \frac{1}{2} m_{\text{b,e}} \left(\mathbf{v}_{\text{e}}^{(\alpha)} \right)^2 \\ &+ \sum_{\gamma=1}^{n_p} \frac{1}{2} m_{\text{b,p}} \left(\mathbf{v}_{\text{p}}^{(\gamma)} \right)^2 + U_{\text{RP}}(\mathbf{r}). \end{aligned} \quad (\text{S.11})$$

Here, $m_{\text{b,e}}$ and $m_{\text{b,p}}$ are the fictitious Parrinello-Rahman masses for the electron and proton,

respectively,^{S18} $\mathbf{v} = \left\{ \mathbf{v}_e^{(1)}, \dots, \mathbf{v}_e^{(n_e)}, \mathbf{v}_p^{(1)}, \dots, \mathbf{v}_p^{(n_p)}, \mathbf{V}_1, \dots, \mathbf{V}_N \right\}$ is the velocity vector for the full system in the ring-polymer representation, and

$$\begin{aligned}
U_{\text{RP}}(\mathbf{r}) = & \frac{1}{n_e} \sum_{\alpha=1}^{n_e} \frac{1}{2} m_e \omega_{n_e}^2 \left(\mathbf{q}_e^{(\alpha)} - \mathbf{q}_e^{(\alpha-1)} \right)^2 \\
& + \frac{1}{n_p} \sum_{\gamma=1}^{n_p} \frac{1}{2} m_p \omega_{n_p}^2 \left(\mathbf{q}_p^{(\gamma)} - \mathbf{q}_p^{(\gamma-1)} \right)^2 \\
& + \frac{1}{n_e} \sum_{\gamma=1}^{n_p} \sum_{l=1}^{n_{\text{ep}}} U \left(\mathbf{q}_e^{((\gamma-1)n_{\text{ep}}+l)}, \mathbf{q}_p^{(\gamma)}, \mathbf{Q} \right).
\end{aligned} \tag{S.12}$$

The transmission coefficient in Eq. (S.6) is obtained from the flux-side correlation function,^{S8,S9}

$$\kappa(t) = \frac{\langle \dot{\xi}_0 h(\xi(\mathbf{r}_t) - \xi^\ddagger) \rangle_c}{\langle \dot{\xi}_0 h(\xi_0) \rangle_c}, \tag{S.13}$$

by releasing RPMD trajectories from the equilibrium ensemble constrained to the dividing surface. Here, $h(\xi)$ is the Heaviside function, $\dot{\xi}_0$ is the time-derivative of the collective variable upon initialization of the RPMD trajectory from the dividing surface with the initial velocities sampled from the Maxwell-Boltzmann (MB) distribution, and \mathbf{r}_t is the time-evolved position of the system along the RPMD trajectory.

2 Systems

This section describes both the fully-atomistic representation of the iron bi-imidazoline system and the system-bath representation for condensed phase PCET used to investigate the competing PCET reaction mechanisms.

2.1 Atomistic Representation for PCET

The atomistic representation of the self-exchange PCET reaction in iron bi-imidazoline includes two $\text{Fe}^{\text{III}}(\text{Hbim})$ complexes treated classically, and a transferring proton and

electron, which are both quantized using RPMD; the entire system is solvated in explicit acetonitrile. The atomic coordinates of both iron complexes are obtained from the experimentally obtained crystal structure of $\text{Fe}^{\text{III}}(\text{H}_2\text{bim})$ to maintain symmetry of the PCET reaction.^{S19}

The potential energy function that describes the atomistic representation is given by

$$U(\mathbf{q}_e, \mathbf{q}_p, \mathbf{Q}) = U_{\text{cl}}(\mathbf{Q}) + U_p(\mathbf{q}_p, \mathbf{Q}) + U_e(\mathbf{q}_e, \mathbf{Q}) + U_{\text{ep}}(\mathbf{q}_e, \mathbf{q}_p), \quad (\text{S.14})$$

where \mathbf{Q} is the set of atomic positions for all of the classical nuclei in both the solvent and iron bi-imidazoline complexes.

The interactions between all of the classical nuclei, $U_{\text{cl}}(\mathbf{Q})$, are described by a modified version of the Generalized Amber Force Field (GAFF), in which the united-atom approximation was used for hydrogens bonded to carbons;^{S20} hydrogens bonded to nitrogens are treated explicitly. The modifications to the GAFF are that (i) the parameters for acetonitrile are obtained from the three-site model of Guardia *et. al.*,^{S21} (ii) the charges on the iron centers are chosen to be $q_{\text{Fe}} = 1.65 e$, such that the rate for the concerted PCET reaction is in agreement with experiment, and (iii) the charges on the bi-imidazoline ligands are obtained through the procedure described below.

The steps taken to obtain the atomic charges on the bi-imidazoline ligands are (i) calculate the atomic charges using the CHELPG method on the isolated protonated, H_2bim , and deprotonated, Hbim , ligands in a continuum solvent representation of acetonitrile.^{S22} The geometries of the ligands were optimized at the RHF/6-31G** level of theory invoking C_{2v} and C_s symmetry, respectively. All electronic structure calculations were performed using the Gaussian09 package.^{S23} (ii) The CHELPG charges on the hydrogens bonded to carbons are added to the carbon charges in accordance with the united-atom approximation. (iii) The CHELPG charges of the 12 nitrogen atoms directly bonded to the two iron centers

are evenly shifted such that the total charges of the $\text{Fe}^{\text{III}}(\text{H}_2\text{bim})$ and $\text{Fe}^{\text{III}}(\text{Hbim})$ complexes were +3 and +2, respectively,

$$q_{\text{N}_j} = q_{\text{N}_j}^{\text{CHELPG}} + \frac{3e - q_{\text{Fe}}}{6}, \quad (\text{S.15})$$

where q_{N_j} is the shifted charge on nitrogen atom j , $q_{\text{N}_j}^{\text{CHELPG}}$ is the charge on nitrogen atom j obtained from the CHELPG calculation and q_{Fe} is the charge on an iron atom obtained by fitting the rate for the concerted PCET reaction to the experimental PCET rate as described above; the charges on both iron atoms are equal. The term $3e - q_{\text{Fe}}$ accounts for the difference in the charge on an iron atom used in the simulations and the formal +3 redox state of the iron atoms; this term is divided by six to account for the six nitrogen atoms bonded to each iron atom. Steps (i)-(iii) fully specify the atomic charges of the four bi-imidazoline ligands that do not participate in the hydrogen bond with the transferring proton. The instantaneous atomic charges on the two bi-imidazoline ligands that do participate in the hydrogen bond change between the values corresponding to the H_2bim and Hbim ligands obtained in steps (i)-(iii) depending on the position of the proton as follows^{S24}

$$q_j(r) = (1 - f(r))q_j^{(\text{p})} + f(r)q_j^{(\text{dp})}, \quad (\text{S.16})$$

$$f(r) = \frac{1}{2} \left[1 + \frac{r - r_0}{\sqrt{(r - r_0)^2 + l^2}} \right], \quad (\text{S.17})$$

where q_j , $q_j^{(\text{p})}$, and $q_j^{(\text{dp})}$ are the instantaneous atomic charge, the atomic charge in the protonated H_2bim ligand, and the atomic charge in the deprotonated Hbim ligand associated with nuclei j . The parameter r_0 is given by half the instantaneous distance between the nitrogen atoms that are directly participating in the hydrogen bond with the transferring proton, and $l = 0.125 \text{ \AA}$ is chosen in agreement with previous work.^{S13} The variable r is given by the distance between the transferring proton and the nitrogen atom participating

in the hydrogen bond associated with the same iron complex corresponding to nuclei j . To conserve charge, the charge of the transferring proton, q_p , is given by

$$q_p = 4e - \sum_j q_j, \quad (\text{S.18})$$

where the sum over j runs over all atoms in the system, and the value of $4e$ corresponds to the total charge of the system.

The interaction between the transferring proton and the classical nuclei in the solvent and both iron complexes is given by

$$U_p(\mathbf{q}_p, \mathbf{Q}) = U_{p,\text{coul}}(\mathbf{q}_p, \mathbf{Q}) + U_{p,\text{lj}}(\mathbf{q}_p, \mathbf{Q}) + U_{\text{HB}}(\mathbf{q}_p, \mathbf{Q}_{\text{ND}}, \mathbf{Q}_{\text{NA}}). \quad (\text{S.19})$$

The potentials $U_{p,\text{coul}}(\mathbf{q}_p, \mathbf{Q})$ and $U_{p,\text{lj}}(\mathbf{q}_p, \mathbf{Q})$ correspond to the usual Coulombic and Lennard-Jones interaction between the transferring proton and all of the classical nuclei except for the two nitrogen atoms participating in the hydrogen bond. The potential describing the hydrogen bond between the proton and the two nitrogen atoms is given by an extension of the Azzouz-Borgis model for PT^{S24}

$$U_{\text{HB}}(\mathbf{q}_p, \mathbf{Q}_{\text{ND}}, \mathbf{Q}_{\text{NA}}) = U_{\text{rep}}(\mathbf{Q}_{\text{ND}}, \mathbf{Q}_{\text{NA}}) + D \left[1 - \exp \left(\frac{-n(r_{\text{HD}} - d)^2}{2r_{\text{HD}}} \right) \right] + D \left[1 - \exp \left(\frac{-n(r_{\text{HA}} - d)^2}{2r_{\text{HA}}} \right) \right], \quad (\text{S.20})$$

where

$$U_{\text{rep}}(\mathbf{Q}_{\text{ND}}, \mathbf{Q}_{\text{NA}}) = \begin{cases} 4\epsilon \left[\left(\frac{\sigma}{R} \right)^{12} - \left(\frac{\sigma}{R} \right)^6 \right] + \epsilon & R < 2^{1/6}\sigma \\ 0 & R \geq 2^{1/6}\sigma \end{cases}, \quad (\text{S.21})$$

and where \mathbf{Q}_{ND} and \mathbf{Q}_{NA} are the positions of the two nitrogen atoms, one associated with the donor and one with the acceptor complex, respectively. The variables r_{HD} and r_{HA} are the distances between the transferring proton and the nitrogen atoms associated with the donor and acceptor complexes, respectively. The parameters $D = 93$ kcal/mol, $n = 11 \text{ \AA}^{-1}$ and $d = 1 \text{ \AA}$ are chosen from common experimental values for nitrogen-proton bonds.^{S25,S26} The potential $U_{\text{rep}}(\mathbf{Q}_{\text{ND}}, \mathbf{Q}_{\text{NA}})$ accounts for the core repulsion between the two nitrogen atoms, where $R = |\mathbf{Q}_{\text{ND}} - \mathbf{Q}_{\text{NA}}|$ is the distance between the two nitrogen atoms and $\epsilon = 250$ kcal/mol and $\sigma = 2.39 \text{ \AA}$ are chosen such that the average distance between the two nitrogen atoms in the simulations corresponds to the distance in the experimental crystal structure of 2.67 \AA .^{S19}

The interaction between the transferring electron and the classical nuclei in the solvent and both iron complexes is given by

$$U_e(\mathbf{q}_e, \mathbf{Q}) = U_{e,\text{coul}}(\mathbf{q}_e, \mathbf{Q}) + U_{e,\text{rep}}(\mathbf{q}_e, \mathbf{Q}). \quad (\text{S.22})$$

The potential $U_{e,\text{coul}}(\mathbf{q}_e, \mathbf{Q})$ describes the scaled pairwise pseudopotential between the electron and the classical nuclei in the solvent and both iron complexes^{S27}

$$U_{e,\text{coul}}(\mathbf{q}_e, \mathbf{Q}) = \sum_{i \in \text{solv}} U_{e-\text{solv}}^i(r_i) + \sum_{j \in \text{cmplx}} U_{e-\text{cmplx}}^j(r_j), \quad (\text{S.23})$$

where $r_i = |\mathbf{q}_e - \mathbf{Q}_i|$ and $r_j = |\mathbf{q}_e - \mathbf{Q}_j|$. The atom index i corresponds to nuclei only in the solvent, and j corresponds to nuclei only in the iron complexes. For cases in which the atom index i corresponds to a positively charged atom,

$$U_{e-\text{solv}}^i(r_i) = \begin{cases} -\zeta_{\text{solv}} \frac{q_i e}{4\pi\epsilon_0 r_{\text{cut}}^i}, & r \leq r_{\text{cut}}^i \\ -\zeta_{\text{solv}} \frac{q_i e}{4\pi\epsilon_0 r_i}, & r > r_{\text{cut}}^i \end{cases}, \quad (\text{S.24})$$

and when i corresponds to a negatively charged atom,

$$U_{\text{e-solv}}^i(r_i) = -\zeta_{\text{solv}} \frac{q_i e}{4\pi\epsilon_0 r_i}. \quad (\text{S.25})$$

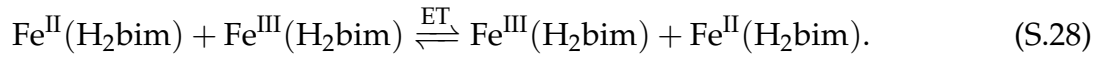
Similarly, when j corresponds to a positively charged atom,

$$U_{\text{e-cmplx}}^j(r_j) = \begin{cases} -\zeta_{\text{cmplx}} \frac{q_j e}{4\pi\epsilon_0 r_{\text{cut}}^j}, & r \leq r_{\text{cut}}^j \\ -\zeta_{\text{cmplx}} \frac{q_j e}{4\pi\epsilon_0 r_j}, & r > r_{\text{cut}}^j \end{cases}, \quad (\text{S.26})$$

and when j corresponds to a negatively charged atom,

$$U_{\text{e-cmplx}}^j(r_j) = -\zeta_{\text{cmplx}} \frac{q_j e}{4\pi\epsilon_0 r_j}. \quad (\text{S.27})$$

The value of the scaling parameter $\zeta_{\text{solv}} = 0.74$ is chosen such that the atomistic representation reproduces $\lambda_0 = 17.9$ kcal/mol, the previously calculated value for the solvent reorganization energy of the symmetric self-exchange ET reaction^{S19}



The value of the scaling parameter $\zeta_{\text{cmplx}} = 0.56$ is chosen such that the atomistic representation reproduces the experimental driving force at the reactive configuration for the formation of the PCET charge separated intermediate, $\Delta G^{\circ'} = 11$ kcal/mol.^{S19}

The potential $U_{\text{e,rep}}(\mathbf{q}_e, \mathbf{Q})$ describes an additional pseudopotential used to model the repulsion between the transferring electron and the electron cloud associated with each nuclei^{S2,S28}

$$U_{\text{e,rep}}(\mathbf{q}_e, \mathbf{Q}) = \sum_{k \notin \text{Fe,H}} \frac{A}{r_k^4} \left[\frac{B}{(C + r_k^6)} - 1 \right], \quad (\text{S.29})$$

where $r_k = |\mathbf{q}_e - \mathbf{Q}_k|$ and the atomic index k runs over all nuclei except proton and iron atoms. The values of the parameters in Eq. S.29 are $A = 32.2$ kcal/mol \AA^4 , $B = 1956.5$ \AA^6

and $C = 276.86 \text{ \AA}^6$.

The parameters above, which we denote System 1a, fully define an atomistic representation of the PCET reaction in iron bi-imidazoline that represents the original experimental conditions.^{S19} In addition, we further define sets of parameters, which allows for the investigation of the physical interactions that govern the dominant PCET reaction. First, we define an analogous set of parameters to those above, Systems 1b and 1c, but in which the atomic charges on the acetonitrile solvent molecules are varied by a multiplicative factor to model different solvent conditions of varying polarity. Second, we define a set of parameters, Systems 2a-2c, in which (i) the atomic charges on the acetonitrile molecules are varied by a multiplicative factor and (ii) the value of the scaling parameter $\zeta_{\text{cmplx}} = 0.30$ is set to model molecular systems with weaker ligand-mediated electron-proton interaction, such as ruthenium terpyridyl-benzoates and iron tetraphenylporphyrin-benzoates.^{S29-S31}

2.2 System-bath Representation for PCET

In addition to the atomistic representation of the PCET reaction in iron bi-imidazoline presented above, we also employ a co-linear system-bath model for PCET. The system-bath model has been described in detail previously and is thus only summarized below.^{S3}

The model is expressed in the position representation using the potential energy function

$$U(q_e, q_p, q_s, \mathbf{Q}) = U_{\text{sys}}(q_e, q_p, q_s) + U_{\text{B}}(q_s, \mathbf{Q}), \quad (\text{S.30})$$

where $U_{\text{B}}(q_s, \mathbf{Q})$ is the potential energy term associated with the bath coordinates, and

$$\begin{aligned} U_{\text{sys}}(q_e, q_p, q_s) = & U_e(q_e) + U_p(q_p) + U_s(q_s) \\ & + U_{\text{es}}(q_e, q_s) + U_{\text{ps}}(q_p, q_s) \\ & + U_{\text{ep}}(q_e, q_p) \end{aligned} \quad (\text{S.31})$$

is the system potential energy. The scalar coordinates q_e , q_p , and q_s describe the one-dimensional (1D) positions of the electron, proton, and solvent modes, respectively, and \mathbf{Q} is the vector of bath oscillator positions.

The first term in the system potential energy function models the interaction of the transferring electron with its donor and acceptor sites,

$$U_e(q_e) = \begin{cases} a_D q_e^2 + b_D q_e + c_D, & r_D^{\text{out}} \leq q_e \leq r_D^{\text{in}} \\ a_A q_e^2 + b_A q_e + c_A, & r_A^{\text{in}} \leq q_e \leq r_A^{\text{out}} \\ -\mu_e \left[\frac{1}{|q_e - r_D|} + \frac{1}{|q_e - r_A|} \right], & \text{otherwise,} \end{cases} \quad (\text{S.32})$$

where r_D and r_A are the positions of the electron donor and acceptor sites.

The second term in the system potential energy function models the interaction between the transferring proton and its donor and acceptor sites,

$$U_p(q_p) = -\frac{m_p \omega_p^2}{2} q_p^2 + \frac{m_p^2 \omega_p^4}{16 V_0} q_p^4. \quad (\text{S.33})$$

Here, ω_p is the proton vibrational frequency and V_0 is the intrinsic PT barrier height.

The next three terms in the system potential energy function model the solvent potential and the electron- and proton-solvent interactions. Specifically,

$$U_s(q_s) = \frac{1}{2} m_s \omega_s^2 q_s^2, \quad (\text{S.34})$$

$$U_{es}(q_e, q_s) = -\mu_{es} q_e q_s, \quad (\text{S.35})$$

and

$$U_{ps}(q_p, q_s) = -\mu_{ps} q_p q_s, \quad (\text{S.36})$$

where m_s is the solvent mass and ω_s is the effective frequency of the solvent coordinate.

Interactions between the transferring electron and proton are modeled via the capped coulombic potential

$$U_e(q_e) = \begin{cases} -\frac{\mu_{ep}}{|q_e - q_p|}, & |q_e - q_p| > R_{\text{cut}} \\ -\frac{\mu_{ep}}{R_{\text{cut}}}, & \text{otherwise.} \end{cases} \quad (\text{S.37})$$

The potential energy term $U_B(q_s, \mathbf{Q})$ models the harmonic bath that is coupled to the PCET reaction. The bath exhibits an ohmic spectral density $J(\omega)$ with cutoff frequency ω_c ,^{S32,S33} such that

$$J(\omega) = \eta \omega e^{-\omega/\omega_c}, \quad (\text{S.38})$$

where η denotes the friction coefficient. The continuous spectral density is discretized into f oscillators with frequencies^{S8,S34}

$$\omega_j = -\omega_c \ln\left(\frac{j-0.5}{f}\right) \quad (\text{S.39})$$

and coupling constants

$$c_j = \omega_j \left(\frac{2\eta M \omega_c}{f\pi}\right)^{1/2}, \quad (\text{S.40})$$

such that

$$U_B(q_s, \mathbf{Q}) = \sum_{j=1}^f \left[\frac{1}{2} M \omega_j^2 \left(Q_j - \frac{c_j q_s}{M \omega_j^2} \right)^2 \right]. \quad (\text{S.41})$$

Here, M is the mass of each bath oscillator, and ω_j and Q_j are the respective frequency and position for the j th oscillator.

We have developed system parameters to model condensed-phase PCET reactions that transition between the concerted and sequential mechanisms. Specifically, Systems 3a-3e vary the strength of the solvent-proton and solvent-electron interactions, Systems 4a-4e

vary the strength of the electron-proton interaction, and Systems 5a-5e vary the barrier height associated with PT. The parameters associated with the system-bath model of PCET are presented in Tables S1 and S2.

Table S1: Coefficients for the electron potential (Eq. (S.32)) in the System bath model.^a

Coefficient	Value
a_D	0.22663
b_D	2.69336
c_D	4.94560
r_D^{in}	-4.0
r_D^{out}	-8.0

^aThe parameters for the acceptor Coulombic well are given by $a_A = a_D$, $b_A = -b_D$, $c_A = c_D$, $r_A^{\text{in}} = -r_D^{\text{in}}$, and $r_A^{\text{out}} = -r_D^{\text{out}}$. All values are reported in atomic units.

Table S2: Parameters for the system-bath model of PCET.^a

Parameter	Systems 3a-3e	Systems 4a-4e	Systems 5a-5e
f	12	12	12
ω_s	2.3221×10^{-4}	2.3221×10^{-4}	2.3221×10^{-4}
ω_c	2.3221×10^{-4}	2.3221×10^{-4}	2.3221×10^{-4}
M	25539	25539	25539
m_s	25539	25539	25539
m_e	1.0	1.0	1.0
m_p	1836.1	1836.1	1836.1
$\eta / M\omega_c$	1.0	1.0	1.0
r_D	-6.0	-6.0	-6.0
r_A	6.0	6.0	6.0
μ_e	3.668	3.668	3.668
ω_p	1.47×10^{-2}	1.47×10^{-2}	$6.00 \times 10^{-3} - 1.59 \times 10^{-2}$
V_0	3.00×10^{-2}	3.00×10^{-2}	$1.50 \times 10^{-2} - 3.50 \times 10^{-2}$
μ_{es}	$-7.80 \times 10^{-4} - -1.26 \times 10^{-3}$	-1.20×10^{-3}	-1.20×10^{-3}
μ_{ps}	$3.90 \times 10^{-3} - 6.30 \times 10^{-3}$	6.00×10^{-3}	6.00×10^{-3}
μ_{ep}	1.1	1.0 - 1.5	1.1

^aAll values are reported in atomic units.

3 Calculation details

3.1 Atomistic representation

The atomistic simulations for all Systems (Systems 1a-1c and Systems 2a-2c) are implemented in the DL_POLY molecular dynamics package, and include 410 acetonitrile molecules.^{S35} In all simulations, the RPMD equations of motion are evolved using the velocity Verlet algorithm.^{S36} The electron is quantized with $n_e = 1024$ ring-polymer beads, and the proton is quantized with $n_p = 32$ ring-polymer beads. As in previous RPMD simulations, each time step for the electron and proton involves separate coordinate updates due to forces arising from the physical potential and due to exact evolution of the purely harmonic portion of the ring-polymer potentials.^{S37} The temperature is set to the experimental value of 298 K.^{S19} All pair-wise interactions are truncated at a distance of $r_{pw} = 12$ Å. Long-range electrostatics, including the Coulombic interactions between classical nuclei, the Coulombic interaction between the proton and the classical nuclei ($U_{p,coul}$), and the Coulombic interactions between the electron and the classical nuclei ($U_{e,coul}$), are treated with the force-shifting algorithm,^{S38} in which the Coulombic potential is multiplied by a damping function $S(r)$, such that both the potential and its derivative smoothly vanish at $r = r_{pw}$, where here r defines the distance between the two particles participating in the pair-wise Coulombic interaction. Specifically,

$$S(r) = \begin{cases} 1 - \frac{2r}{r_{pw}} + \frac{r^2}{r_{pw}^2}, & r \leq r_{pw} \\ 0, & r > r_{pw}. \end{cases} \quad (\text{S.42})$$

All atomistic calculations are performed in a rectangular simulation cell with periodic boundary conditions. The side-lengths of the cell for each System are obtained from 1.5 ns NPT equilibrium simulations run with the Nosé-Hoover barostat and thermostat using a thermostat and barostat relaxation time of 1.0 ps and 2.0 ps, respectively. The side-lengths of the cell for each System are presented in Table S3.

Table S3: Side-lengths of the simulation cell for the atomistic representation of PCET.^a

System	L_1	L_2	L_3
1a	29.498	29.498	45.221
1b	28.778	28.778	44.116
1c	28.179	28.170	43.198
2a	30.236	30.236	46.352
2b	29.498	29.498	45.221
2c	29.103	29.103	44.116

^aThe parameters are given in Å, where L_1 , L_2 , and L_3 are the three sides of the rectangular simulation cell.

3.1.1 Collective variables

Several collective variables are used to monitor and characterize the PCET reaction in the atomistic representation. The progress of the electron is characterized by a “bead-count” coordinate, θ_e , that reports on the fraction of ring-polymer beads that are located on the iron atom associated with the donor complex,

$$\theta_e \left(\mathbf{q}_e^{(1)}, \dots, \mathbf{q}_e^{(n_e)}, \mathbf{Q}_{\text{FeD}}, \mathbf{Q}_{\text{FeA}} \right) = \frac{1}{n_e} \sum_{\alpha=1}^{n_e} \tanh \left(\frac{\phi}{\theta_{\text{FeD}}} \theta^{(\alpha)} \right), \quad (\text{S.43})$$

where

$$\theta_{\text{FeD}} (\mathbf{Q}_{\text{FeD}}, \mathbf{Q}_{\text{FeA}}) = -\frac{1}{2} |\mathbf{Q}_{\text{FeA}} - \mathbf{Q}_{\text{FeD}}| \quad (\text{S.44})$$

and

$$\theta^{(\alpha)} \left(\mathbf{q}_e^{(1)}, \dots, \mathbf{q}_e^{(n_e)}, \mathbf{Q}_{\text{FeD}}, \mathbf{Q}_{\text{FeA}} \right) = \left(\mathbf{q}^{(\alpha)} - \frac{1}{2} (\mathbf{Q}_{\text{FeA}} + \mathbf{Q}_{\text{FeD}}) \right) \cdot \left(\frac{1/2 (\mathbf{Q}_{\text{FeA}} - \mathbf{Q}_{\text{FeD}})}{|1/2 (\mathbf{Q}_{\text{FeA}} - \mathbf{Q}_{\text{FeD}})|} \right) \quad (\text{S.45})$$

The variables \mathbf{Q}_{FeD} , and \mathbf{Q}_{FeA} are the positions of the iron atoms associated with the donor and acceptor complex, respectively, and $\phi = -3.0$.

The progress of the proton is characterized by the difference between the distances of the ring-polymer centroid and the position of the two nitrogen atoms participating in the

hydrogen bond,

$$\theta_p \left(\mathbf{q}_p^{(1)}, \dots, \mathbf{q}_p^{(n_p)}, \mathbf{Q}_{ND}, \mathbf{Q}_{NA} \right) = |\mathbf{Q}_{ND} - \bar{\mathbf{q}}_p| - |\mathbf{Q}_{NA} - \bar{\mathbf{q}}_p|, \quad (\text{S.46})$$

where

$$\bar{\mathbf{q}}_p \left(\mathbf{q}_p^{(1)}, \dots, \mathbf{q}_p^{(n_p)} \right) = \frac{1}{n_p} \sum_{\gamma=1}^{n_p} \mathbf{q}_p^{(\gamma)}. \quad (\text{S.47})$$

The progress of the solvent during the concerted PCET reaction is characterized by the energy gap associated with the transfer of both the electron and proton,

$$\begin{aligned} \Delta U(\mathbf{Q}) = & \frac{-e}{4\pi\epsilon_0} \sum_{i \in \text{solv}} \left[\zeta_{\text{solv}} \left(\frac{q_i}{|\mathbf{Q}_i - \mathbf{Q}_{\text{FeA}}|} - \frac{q_i}{|\mathbf{Q}_i - \mathbf{Q}_{\text{FeD}}|} \right) \right. \\ & \left. + \sum_{j \in \text{cmplx}} \left(\frac{q_i q_j^{\text{A}}}{|\mathbf{Q}_i - \mathbf{Q}_j|} - \frac{q_i q_j^{\text{D}}}{|\mathbf{Q}_i - \mathbf{Q}_j|} \right) \right], \end{aligned} \quad (\text{S.48})$$

where q_j^{D} and q_j^{A} are the atomic charges associated with nuclei j when the proton is bonded to the donor or acceptor complex, respectively. Thus, $q_j^{\text{D}} = q_j^{(\text{p})}$ and $q_j^{\text{A}} = q_j^{(\text{dp})}$ if j is associated with the donor complex; $q_j^{\text{D}} = q_j^{(\text{dp})}$ and $q_j^{\text{A}} = q_j^{(\text{p})}$ if j is associated with the acceptor complex.

The progress of the solvent during the ET step in the sequential mechanism and during the single ET reaction (Eq. (S.28)) is characterized by the energy gap associated with just the transfer of the electron,

$$\Delta U^{\text{ET}}(\mathbf{Q}) = \frac{-e}{4\pi\epsilon_0} \sum_{i \in \text{solv}} \zeta_{\text{solv}} \left(\frac{q_i}{|\mathbf{Q}_i - \mathbf{Q}_{\text{FeA}}|} - \frac{q_i}{|\mathbf{Q}_i - \mathbf{Q}_{\text{FeD}}|} \right). \quad (\text{S.49})$$

The time-dependent dipole of the iron bi-imidazoline complexes pictured in Fig. 6 of

the main text are defined as follows

$$d_e(t) = \left\langle \frac{-1}{n_e} \sum_{\alpha=1}^{n_e} ex^{(\alpha)}(t) \right\rangle_{\text{traj}}, \quad (\text{S.50})$$

$$d_p(t) = \left\langle \frac{1}{n_p} \sum_{\gamma=1}^{n_p} q_p(t) x^{(\gamma)}(t) \right\rangle_{\text{traj}}, \quad (\text{S.51})$$

$$d_{\text{lig}}(t) = \left\langle \sum_{j \in \text{lig}} q_k(t) x_j(t) \right\rangle_{\text{traj}}, \quad (\text{S.52})$$

and

$$d_{\text{tot}}(t) = d_e(t) + d_p(t) + d_L(t), \quad (\text{S.53})$$

where $\langle \dots \rangle_{\text{traj}}$ denotes the non-equilibrium ensemble average over the time-evolved reactive RPMD trajectories for concerted PCET; the non-equilibrium average is calculated according to the protocol described below in the RPMD transition path ensemble section. The variable $x_j(t)$ is calculated as

$$x_j(t) = \left(\frac{\mathbf{Q}_{\text{FeA}} - \mathbf{Q}_{\text{FeD}}}{|\mathbf{Q}_{\text{FeA}} - \mathbf{Q}_{\text{FeD}}|} \right) \cdot (\mathbf{Q}_j - \mathbf{Q}_{\text{com}}), \quad (\text{S.54})$$

where \mathbf{Q}_{com} is the position of the center of mass of the reactive species, which includes the nuclei in both iron complexes, the electron ring-polymer, and the proton ring-polymer. The variables $x^{(\alpha)}$ and $x^{(\gamma)}$ are defined analogously to Eq. (S.54), where the position of the electron ring-polymer bead α , or the proton ring-polymer bead γ , is substituted for \mathbf{Q}_j , respectively.

3.1.2 RPMD rate calculations for concerted PCET

The rate constant for the bimolecular (second-order) concerted PCET reaction may be expressed as^{S26,S39,S40}

$$k_{\text{bi}} = K_{\text{A}}(r)k_{\text{uni}}, \quad (\text{S.55})$$

where K_{A} is the equilibrium constant for the formation of the precursor complex at a separation distance between the two iron atoms, r , and $k_{\text{uni}}^{\text{CPET}}$ is the uni-molecular (first-order) rate constant for the concerted PCET reaction. The equilibrium constant is expressed as

$$K_{\text{A}}(r) = P_{\text{r}} \exp(-\beta w_{\text{r}}), \quad (\text{S.56})$$

where w_{r} is the work to bring the two reacting iron complexes together. The prefactor P_{r} can be approximated as

$$P_{\text{r}} = 4\pi N_{\text{A}} r^2 \delta r \times 10^{-27}, \quad (\text{S.57})$$

where δr is the range of iron-iron distances over which the rate is appreciable. Here, P_{r} is given in units of inverse moles per liter, and r and δr are given in angstroms. In this paper, $r = 10.3 \text{ \AA}$ is given by the iron-iron distance in the crystal structure of $\text{Fe}^{\text{III}}\text{Hbim}$, $\delta r = 0.8 \text{ \AA}$, which has shown to provide reasonable results,^{S26,S40} and $w_{\text{r}} = 1.35 \text{ kcal mol}^{-1}$ has been previously calculated.^{S19,S26}

The unimolecular rate, k_{uni} is calculated using RPMD from the product of the TST rate and the transmission coefficient (Eq. (S.5)). The FE profiles that appear in the TST rate expression, Eq. (S.6), are obtained using umbrella sampling as described below.

For all atomistic systems, the 1D FE profile used in the concerted PCET rate calculation is obtained in the electron bead-count coordinate, $F(\theta_{\text{e}})$, using the following umbrella sampling protocol; the 1D FE profile corresponding to the experimental conditions (System 1a) is presented in Fig. 4a in the main text. Forty-five independent sampling trajectories are harmonically restrained to uniformly spaced values of θ_{e} in the region $[0.0, 0.88]$

using a force constant of 10,000 kcal/mol; six independent sampling trajectories are harmonically restrained to uniformly spaced values of θ_e in the region $[0.90, 0.95]$ using a higher force constant of 20,000 kcal/mol; two independent sampling trajectories are harmonically restrained to uniformly spaced values of θ_e in the region $[0.96, 0.97]$ using a higher force constant of 40,000 kcal/mol; ten independent sampling trajectories are harmonically restrained to uniformly spaced values of θ_e in the region $[0.98, 0.998]$ using a higher force constant of 1×10^6 kcal/mol; an additional independent sampling trajectory is harmonically restrained to a value of $\theta_e = 0.989$ using a force constant of 1×10^6 kcal/mol to ensure extensive overlap among the sampled distributions. The symmetry of the reaction is employed to obtain the full FE profile along θ_e over the region $[-0.998, 0.998]$. For all Systems, an auxiliary restraining potential is introduced to the sampling trajectories to restrict the system to the concerted channel, as described in a following section. The equilibrium sampling trajectories are performed using path-integral molecular dynamics (PIMD) with $m_{b,e} = 5.357$ g/mol and $m_{b,p} = 3.156$ g/mol, which allows for a timestep of 1 fs. Each sampling trajectory is run for at least 1 ns, and thermostating is performed by re-sampling the velocities from the MB distribution every 3 ps. It is important to note, that as always, the choice of the Parinello-Rahman masses, $m_{b,e}$ and $m_{b,p}$, allows for a large time step in the sampling trajectories, but has no affect of $F(\theta_e)$ or any other equilibrium ensemble average.^{S18,S37,S41}

For all atomistic Systems, the transmission coefficient is calculated using RPMD trajectories that are released from the dividing surface associated with $\theta_e = 0$. At least 3000 trajectories are released for each system. Each RPMD trajectory is evolved for 300 fs using a timestep of 5×10^{-4} fs and with initial velocities sampled from the MB distribution. Initial configurations for the RPMD trajectories are selected every 1 ps from long PIMD sampling trajectories that are constrained to the dividing surface using the RATTLE algorithm.^{S42} The sampling trajectories utilize $m_{b,e} = 5.357$ g/mol, $m_{b,p} = 3.156$ g/mol, and a time-step of 1 fs. Thermostating is performed by re-sampling the velocities from the MB distribution

every 3 ps. For all Systems, the same auxiliary potential used in the calculation of $F(\theta_e)$ is introduced for the PIMD sampling trajectories to restrict the system to the concerted channel; throughout this paper, the PRMD trajectories used to calculate the transmission coefficients are not subject to any auxiliary restraining potentials.

3.1.3 RPMD rate calculations for ET prior to PT

For all atomistic systems, we calculate the rate for the ET prior to PT step in the sequential mechanism corresponding to the forward rate of Eq. 5 in the main text. The bimolecular rate constant for the ET prior to PT step is given by the same expression as for the concerted reaction, Eq. (S.55). The value of $K_A(r)$ is the same as for the concerted reaction since the reactant species are identical between the ET prior to PT and concerted reactions. The unimolecular rate for the ET prior to PT step is also calculated using RPMD from the product of the product of the TST rate and the transmission coefficient, Eq. (S.5).

The 1D FE profile used in the rate calculation for the ET reactions is obtained in the electron bead-count coordinate, $F(\theta_e)$, using the following umbrella sampling protocol; the 1D FE profile corresponding to the ET reaction under experimental conditions (System 1a) is presented in Fig. 4b in the main text. Eighty-nine independent sampling trajectories are harmonically restrained to uniformly spaced values of θ_e in the region $[-0.88, 0.88]$ using a force constant of 10000 kcal/mol; six independent sampling trajectories are harmonically restrained to uniformly spaced values of θ_e in the both the region $[-0.95, -0.90]$ and $[0.90, 0.95]$ using a higher force constant of 20000 kcal/mol; two independent sampling trajectories are harmonically restrained to uniformly spaced values of θ_e in the both the region $[-0.97, -0.96]$ and $[0.96, 0.97]$ using a higher force constant of 40000 kcal/mol; ten independent sampling trajectories are harmonically restrained to uniformly spaced values of θ_e in both the region $[-0.998, 0.98]$ and $[0.98, 0.998]$ using a higher force constant of 1×10^6 kcal/mol; two additional independent sampling trajectories are harmonically restrained to the values of $\theta_e = 0.989$ and $\theta_e = -0.989$ using a force constant of 1×10^6

kcal/mol. For all Systems, an auxiliary restraining potential is introduced to the sampling trajectories to restrict the system to the ET channel, as described in a following section. As before, the PIMD sampling trajectories employ $m_{b,e} = 5.357$ g/mol, $m_{b,p} = 3.156$ g/mol, and a time-step of 1 fs. Thermostatting is performed by re-sampling the velocities from the MB distribution every 3 ps, and each trajectory is run for at least 1 ns.

The transmission coefficient is calculated using RPMD trajectories that are released from the dividing surface associated with $\theta_e = 0.62$. At least 3000 trajectories are released for each system. Each RPMD trajectory is evolved for 300 fs using a timestep of 5×10^{-4} fs and with initial velocities sampled from the MB distribution. Initial configurations for the RPMD trajectories are selected every 1 ps from long PIMD sampling trajectories that are constrained to the dividing surface using the RATTLE algorithm.^{S42} The sampling trajectories utilize $m_{b,e} = 5.357$ g/mol, $m_{b,p} = 3.156$ g/mol, and a time-step of 1 fs. Thermostatting is performed by re-sampling the velocities from the MB distribution every 3 ps. For all Systems, the same auxiliary potential used in the calculation of $F_{\text{SET}}(\theta_e)$ is introduced for the PIMD sampling trajectories to restrict the system to the concerted channel, as described in Appendix 4.2

3.1.4 1D FE profile for PT prior to ET

For the experimental conditions (System 1a), we calculate the FE profile for the PT step in the sequential mechanism corresponding to the reaction in Eq. 6 of the main text. The 1D FE profile is obtained in the proton collective variable, $F(\theta_p)$, using the following umbrella sampling protocol. Fifteen independent sampling trajectories are harmonically restrained to uniformly spaced values of θ_p in the region $[-0.35 \text{ \AA}, 0.35 \text{ \AA}]$ using a force constant of 1000 kcal/mol \AA^{-2} and seven independent sampling trajectories are harmonically restrained to uniformly spaced values of θ_p in both the region $[-0.70 \text{ \AA}, -0.40 \text{ \AA}]$ and $[0.40 \text{ \AA}, 0.70 \text{ \AA}]$ using a force constant of 500 kcal/mol \AA^{-2} . The PIMD sampling trajectories employ $m_{b,e} = 5.357$ g/mol, $m_{b,p} = 3.156$ g/mol, and a time-step of 1 fs. Thermostatting is performed by

re-sampling the velocities from the MB distribution every 3 ps, and each trajectory is run for 500 ps. In addition, the electron ring-polymer is initialized to the position of the iron atom associated with the donor iron bi-imidazoline complex for each sampling trajectory, though no additional restraint on the electron ring-polymer is introduced. The FE profile is presented in Fig. 4c in the main text; based on the symmetry of the reaction, the PT prior to ET and PT following ET steps are equivalent.

3.1.5 Two-dimensional FE profiles

We calculate the two-dimensional (2D) FE profile for System 1a in the electron bead-count and proton coordinates, $F(\theta_e, \theta_p)$, as presented in Fig. 3 in the main text. The 2D FE profile is constructed using PIMD sampling trajectories that are harmonically restrained in both the θ_e and θ_p coordinates. A total of 1856 sampling trajectories are performed, in which the coordinates θ_e and θ_p are sampled using a square grid. The coordinate θ_e is sampled using forty-five independent sampling trajectories that are harmonically restrained to uniformly spaced values of θ_e in the region $[0.0, 0.88]$ using a force constant of 10,000 kcal/mol; six independent sampling trajectories are harmonically restrained to uniformly spaced values of θ_e in the region $[0.90, 0.95]$ using a higher force constant of 20,000 kcal/mol; two independent sampling trajectories are harmonically restrained to uniformly spaced values of θ_e in the region $[0.96, 0.97]$ using a higher force constant of 40,000 kcal/mol; ten independent sampling trajectories are harmonically restrained to uniformly spaced values of θ_e in the region $[0.98, 0.998]$ using a higher force constant of 1×10^6 kcal/mol; an additional independent sampling trajectory is harmonically restrained to a value of $\theta_e = 0.989$ using a force constant of 1×10^6 kcal/mol. The symmetry of the reaction is employed to obtain the full FE profile along θ_e over the region $[-0.998, 0.998]$. The coordinate θ_p is sampled using fifteen independent sampling trajectories that are harmonically restrained to uniformly spaced values of θ_p in the region $[-0.35 \text{ \AA}, 0.35 \text{ \AA}]$ using a force constant of $1000 \text{ kcal/mol \AA}^{-2}$ and seven independent sampling trajectories

are harmonically restrained to uniformly spaced values of θ_p in both the region $[-0.70 \text{ \AA}, -0.40 \text{ \AA}]$ and $[0.40 \text{ \AA}, 0.70 \text{ \AA}]$ using a force constant of $500 \text{ kcal/mol \AA}^{-2}$. No auxiliary restraining potentials are employed for the calculation of $F(\theta_e, \theta_p)$. The PIMD sampling trajectories employ $m_{b,e} = 5.357 \text{ g/mol}$, $m_{b,p} = 3.156 \text{ g/mol}$, and a time-step of 1 fs . Thermostatting is performed by re-sampling the velocities from the MB distribution every 3 ps , and each trajectory is run for 500 ps .

We additionally calculate the 2D FE profile for System 1a in the electron bead-count and concerted PCET energy gap coordinates, $F(\theta_e, \Delta U)$, for sampling trajectories corresponding to the concerted PCET reaction, as presented in Fig. 5 in the main text. To generate $F(\theta_e, \Delta U)$, the harmonically restrained sampling trajectories used to calculate $F(\theta_e)$ for System 1a are utilized.

3.1.6 Solvent reorganization energy for concerted PCET

For Systems 1a-1c, we calculate the solvent reorganization energy associated with concerted PCET in the tight-binding approximation, which is a well-defined and standard definition.^{S14,S27,S43} This yields a single reorganization energy, which is appropriate for the path-integral formulation of the rate theory employed in this work and distinct from the Fermi Golden Rule treatment of PCET.^{S44,S45} The solvent reorganization energy is calculated using the equation^{S14,S27,S43}

$$\lambda_o^{\text{CPET}} = F_D^{\text{CPET}}(\Delta U_A) - F_D^{\text{CPET}}(\Delta U_D), \quad (\text{S.58})$$

where ΔU_D and ΔU_A correspond to the minimum value of ΔU in the FE profiles $F_D^{\text{CPET}}(\Delta U)$ and $F_A^{\text{CPET}}(\Delta U)$, corresponding to the electron and proton being associated with the donor or acceptor, respectively. The 1D FE profiles $F_D^{\text{CPET}}(\Delta U)$ and $F_A^{\text{CPET}}(\Delta U)$ are calculated along the energy gap coordinate, ΔU , using the following umbrella sampling protocol. The coordinate ΔU is sampled using seventeen independent sampling trajectories that are

harmonically restrained to uniformly spaced values of ΔU in the region [-40 kcal/mol,40 kcal/mol] using a force constant of 1.20×10^{-6} kcal/mol (kcal/mol) $^{-2}$. The sampling trajectories used to calculate the FE profile $F_D^{\text{CPET}}(\Delta U)$ and $F_A^{\text{CPET}}(\Delta U)$ are initialized with the electron and proton associated with the donor or acceptor iron bi-imidazoline complex, respectively. The PIMD sampling trajectories employ $m_{b,e} = 5.357$ g/mol, $m_{b,p} = 3.156$ g/mol and a time-step of 1 fs. Thermostatting is performed by re-sampling the velocities from the MB distribution every 3 ps, and each trajectory is run for 1 ns.

3.1.7 Solvent reorganization energy for ET prior to PT

For Systems 1a-1c , we calculate the solvent reorganization energy associated with the ET reaction prior to PT in the sequential mechanism in the tight-binding approximation from the equation^{S14,S27,S43}

$$\lambda_o^{\text{ETPT}} = F_D^{\text{ETPT}}(\Delta U_A^{\text{ET}}) - F_D^{\text{ETPT}}(\Delta U_D^{\text{ET}}), \quad (\text{S.59})$$

where ΔU_D^{ET} and ΔU_A^{ET} correspond to the minimum value of ΔU^{ET} in the FE profiles $F_D^{\text{ETPT}}(\Delta U^{\text{ET}})$ and $F_A^{\text{ETPT}}(\Delta U^{\text{ET}})$, corresponding to the electron being associated with the donor or acceptor, respectively. The 1D FE profiles $F_D^{\text{ETPT}}(\Delta U^{\text{ET}})$ and $F_A^{\text{ETPT}}(\Delta U^{\text{ET}})$ are calculated along the energy gap coordinate, ΔU^{ET} , using the following umbrella sampling protocol. The coordinate ΔU^{ET} is sampled using seventeen independent sampling trajectories that are harmonically restrained to uniformly spaced values of ΔU^{ET} in the region [-40 kcal/mol,40 kcal/mol] using a force constant of 1.20×10^{-6} kcal/mol (kcal/mol) $^{-2}$. The sampling trajectories used to calculate the FE profile $F_D^{\text{ETPT}}(\Delta U^{\text{ET}})$ and $F_A^{\text{ETPT}}(\Delta U^{\text{ET}})$ are initialized with the electron ring-polymer at the position of the iron atom associated with the donor or acceptor iron bi-imidazoline complex, respectively; for the calculation of both FE profiles the proton is associated with the donor iron bi-imidazoline complex and an auxiliary restraining potential is introduced to the sampling trajectories to restrict the

system to the ET channel, as described in Appendix 4.2. The PIMD sampling trajectories employ $m_{b,e} = 5.357$ g/mol, $m_{b,p} = 3.156$ g/mol and a time-step of 1 fs. Thermostatting is performed by re-sampling the velocities from the MB distribution every 3 ps, and each trajectory is run for 1 ns.

3.1.8 Solvent reorganization energy for symmetric ET

For the calculation of the parameter ζ_{solv} as described in the Systems section, we additionally calculate the solvent reorganization energy associated with the single ET reaction (Eq. (S.28)) in the tight-binding approximation from the equation^{S14,S27,S43}

$$\lambda_o^{\text{ETPT}} = F_D^{\text{ETPT}}(\Delta U_A^{\text{ET}}) - F_D^{\text{ETPT}}(\Delta U_D^{\text{ET}}), \quad (\text{S.60})$$

where ΔU_D^{ET} and ΔU_A^{ET} correspond to the minimum value of ΔU^{ET} in the FE profiles $F_D^{\text{ET}}(\Delta U^{\text{ET}})$ and $F_A^{\text{ET}}(\Delta U^{\text{ET}})$, corresponding to the electron being associated with the donor or acceptor, respectively. The 1D FE profiles $F_D^{\text{ETPT}}(\Delta U^{\text{ET}})$ and $F_A^{\text{ETPT}}(\Delta U^{\text{ET}})$ are calculated along the energy gap coordinate, ΔU^{ET} , using the following umbrella sampling protocol. The coordinate ΔU^{ET} is sampled using seventeen independent sampling trajectories that are harmonically restrained to uniformly spaced values of ΔU^{ET} in the region [-40 kcal/mol, 40 kcal/mol] using a force constant of 1.20×10^{-6} kcal/mol (kcal/mol)⁻². The sampling trajectories used to calculate the FE profile $F_D^{\text{ET}}(\Delta U^{\text{ET}})$ and $F_A^{\text{ET}}(\Delta U^{\text{ET}})$ involve two fully protonated Fe^{III}(H₂bim) complexes, in which all protons are treated classically and the electron ring-polymer is initialized to the position of the iron atom associated with the donor or acceptor iron bi-imidazoline complex, respectively. The PIMD sampling trajectories employ $m_{b,e} = 5.357$ g/mol and a time-step of 1 fs. Thermostatting is performed by re-sampling the velocities from the MB distribution every 3 ps, and each trajectory is run for 1 ns.

3.1.9 RPMD transition path ensemble

As we have done previously,^{S3,S46} we analyze the transition path ensemble^{S47} for the RPMD trajectories in the current study. Reactive trajectories are generated through forward- and backward-integration of initial configurations drawn from the dividing surface ensemble with initial velocities drawn from the MB distribution. Reactive trajectories correspond to those for which forward- and backward-integrated half trajectories terminated in opposite sides of the dividing surface. The reactive trajectories that are initialized from the equilibrium Boltzmann distribution on the dividing surface must be reweighted to obtain the unbiased transition path ensemble.^{S47-S49} A weighting term, w_α , is applied to each trajectory, correctly accounting for recrossing and for the fact that individual trajectories are performed in the microcanonical ensemble. This term is given by^{S48}

$$w_\alpha = \left(\sum_i |\dot{\xi}(\mathbf{r})_i|^{-1} \right)^{-1}, \quad (\text{S.61})$$

where the sum includes all instances in which trajectory α crosses the dividing surface, and $\dot{\xi}(\mathbf{r})_i$ is the velocity in the dividing surface collective variable at the i^{th} crossing event. The reweighting has a minor effect on the non-equilibrium averages if the reactive trajectories initialized from the dividing surface exhibit relatively little recrossing, as is the case for the systems studied in this paper. Non-equilibrium averages over the RPMD transition path ensemble are calculated by aligning reactive trajectories at time 0, defined as the moment in time when the trajectories are released from the dividing surface.

3.2 System-bath representation

The simulations for the system-bath models of PCET (Systems 3a-3e, Systems 4a-4e, and Systems 5a-5e) are all performed at $T = 300$ K. The RPMD equations of motion are evolved using the velocity Verlet algorithm,^{S36} and each time step for the electron and proton involves separate coordinate updates due to forces arising from the physical potential and

due to exact evolution of the purely harmonic portion of the ring-polymer potentials.^{S37} The electron is quantized with $n_e = 1024$ ring-polymer beads, and the proton is quantized with $n_p = 32$ ring-polymer beads.

3.2.1 Collective Variables

The progress of the electron in the system-bath models is monitored using a 1D form of the electron bead-count coordinate,

$$\theta_e \left(q_e^{(1)}, \dots, q_e^{(n_e)} \right) = \frac{1}{n_e} \sum_{\alpha=1}^{n_e} \tanh \left(\theta q_e^{(\alpha)} \right), \quad (\text{S.62})$$

where $\theta = -3.0/r_D$.

The progress of the proton in the system-bath models is monitored using the ring-polymer centroid in the proton position coordinate,

$$\bar{q}_p \left(q_p^{(1)}, \dots, q_p^{(n_p)} \right) = \frac{1}{n_p} \sum_{\gamma=1}^{n_p} q_p^{(\gamma)}. \quad (\text{S.63})$$

The solvent dipole presented in Fig. 9(a) in the main text is given by

$$\text{Solvent Dipole} = \mu_{\text{es}} \langle \bar{q}_e \rangle_{\text{reac}} + \mu_{\text{ps}} \langle \bar{q}_p \rangle_{\text{reac}}, \quad (\text{S.64})$$

where \bar{q}_e is the centroid of the electron ring polymer and $\langle \dots \rangle_{\text{reac}}$ denotes the equilibrium ensemble average in the reactant basin.

3.2.2 RPMD rate calculations for concerted PCET

As in the atomistic representation for PCET, the RPMD reaction rate in the system-bath models is calculated from the product of the TST rate and the transmission coefficient (Eq. (S.5)). The 1D FE profile used in the rate calculation for the concerted PCET reactions is obtained in the electron bead-count coordinate, $F(\theta_e)$, using the following umbrella

sampling protocol. 93 independent sampling trajectories are harmonically restrained to uniformly spaced values of θ_e in the region $[-0.92, 0.92]$ using a force constant of 20 a.u.; seven independent sampling trajectories are harmonically restrained to uniformly spaced values of θ_e in both the region $[-0.991, -0.985]$ and in $[0.985, 0.991]$ using a higher force constant of 5000 a.u.; nine independent sampling trajectories are harmonically restrained to uniformly spaced values of θ_e in both the region $[-1.0, -0.992]$ and in $[0.992, 1.0]$ using a higher force constant of 10,000 a.u.; 32 independent sampling trajectories are harmonically restrained to the values of $\theta_e \in \{ \pm 0.93, \pm 0.935, \pm 0.94, \pm 0.945, \pm 0.95, \pm 0.955, \pm 0.96, \pm 0.962, \pm 0.965, \pm 0.967, \pm 0.97, \pm 0.974, \pm 0.976, \pm 0.978, \pm 0.98, \pm 0.982 \}$ using a force constant of 500 a.u. For all Systems, an auxiliary restraining potential is introduced for the PIMD sampling trajectories to restrict the system to the concerted channel, as described in a following section. Each sampling trajectory is run for 10 ns using a timestep of 0.1 fs, with $m_{b,e} = 2000$ a.u. and $m_{b,p} = 1836.1$ a.u. Thermostatting is performed by re-sampling the velocities from the MB distribution every 500 fs.

The transmission coefficient is calculated using a total of 6000 RPMD trajectories that are released from the dividing surface associated with $\theta_e = 0$. Each RPMD trajectory is evolved for 300 fs using a timestep of 1×10^{-4} fs and with the initial velocities sampled from the MB distribution. Initial configurations for the RPMD trajectories are selected every 10 ps from long PIMD sampling trajectories that are constrained to the dividing surface. The sampling trajectories employ $m_{b,e} = 2000$ a.u., $m_{b,p} = 1836.1$ a.u., and a timestep of 0.1 fs. Thermostatting is performed by re-sampling the velocities from the MB distribution every 500 fs. The sampling trajectories are constrained to the dividing surface using the RATTLE algorithm. The same auxiliary restraining potential used in the calculation of $F(\theta_e)$ is introduced for the PIMD sampling trajectories to restrict the system to the concerted channel.

3.2.3 RPMD rate calculations for ET prior to PT

We calculate the rate for the forward ET reaction in the sequential PCET mechanism. The 1D FE profile used in the rate calculation for the ET reactions is obtained in the electron bead-count coordinate, $F(\theta_e)$, using the same umbrella sampling protocol described for the calculation of the FE profile associated with the concerted reaction presented above; however, in the calculation of the FE profile for the ET prior to PT reaction, an auxiliary restraining potential is introduced for the PIMD sampling trajectories to restrict the system to the ET channel, as described in a following section. The independent sampling trajectories used to calculate $F_{\text{SET}}(\theta_e)$ are each run for 10 ns.

Table S4: Dividing surfaces for the sequential ET reaction prior to PT in the system-bath models.

System	θ_e^\ddagger
1a	8.00×10^{-1}
1b	3.76×10^{-1}
1c	1.78×10^{-1}
1d	-2.03×10^{-2}
1e	5.63×10^{-2}
2a	8.32×10^{-2}
2b	2.25×10^{-3}
2c	1.30×10^{-1}
2d	1.80×10^{-1}
2e	3.00×10^{-1}
3a	7.88×10^{-2}
3b	5.18×10^{-2}
3c	5.18×10^{-2}
3d	7.88×10^{-2}
3e	6.52×10^{-2}

The transmission coefficients for the forward ET reactions are calculated using RPMD trajectories that are released from the dividing surfaces present in Table S4. A total of 6000 RPMD trajectories are released for each System. Each RPMD trajectory is evolved for 300 fs using a timestep of 1×10^{-4} fs and with the initial velocities sampled from the MB distribution. Initial configurations for the RPMD trajectories are selected every 10 ps

from long PIMD sampling trajectories that are constrained to the dividing surface. The sampling trajectories employ $m_{b,e} = 2000$ a.u., $m_{b,p} = 1836.1$ a.u., and a timestep of 0.1 fs. Thermostatting is performed by re-sampling the velocities from the MB distribution every 500 fs. The sampling trajectories are constrained to the dividing surface using the RATTLE algorithm. The same auxiliary restraining potential used in the calculation of $F(\theta_e)$ is introduced for the PIMD sampling trajectories to restrict the system to the ET channel.

4 Auxiliary restraining potentials

This section describes auxiliary restraining potentials that are introduced for the PIMD sampling trajectories used in the calculation of 1D FE profiles and in the initial sampling of configurations for the RPMD trajectories both in the atomistic and system-bath models of PCET. These auxiliary restraining potentials simply prevent the PIMD sampling trajectories from visiting configurations outside of the sequential or concerted PCET channel of interest.

4.1 Auxiliary restraining potential for concerted PCET in the atomistic models

For Systems 1a-1c and 2a-2c, we now discuss the auxiliary restraining potential introduced to restrict equilibrium sampling of the system to the concerted channel. This potential is given by

$$U_{\text{aux}}(\theta_p, \theta_e) = \begin{cases} a_{\text{aux}} [\theta_p - q_+(\theta_e)]^2, & \theta_p > q_+(\theta_e) \\ a_{\text{aux}} [\theta_p - q_-(\theta_e)]^2, & \theta_p < q_-(\theta_e) \\ 0, & \text{otherwise} \end{cases} \quad (\text{S.65})$$

where

$$q_+(\theta_e) = b_{\text{aux}}\theta_e + c_{\text{aux}} \quad (\text{S.66})$$

and

$$q_-(\theta_e) = b_{\text{aux}}\theta_e - c_{\text{aux}}. \quad (\text{S.67})$$

The coefficients a_{aux} , b_{aux} , and c_{aux} (Table S5) are chosen to restrict the system to the concerted channel.

Table S5: Parameters for the auxiliary restraining potential in Eq. S.65.^a

System	a_{aux}	b_{aux}	c_{aux}
1a	1000	0.50	0.33
1b	1000	0.50	0.33
1c	1000	0.50	0.33
2a	1000	0.48	0.21
2b	1000	0.48	0.19
2c	1000	0.47	0.15

^a a_{aux} is given in units of kcal/mol Å⁻². b_{aux} and c_{aux} are given in units of Å.

4.2 Auxiliary restraining potential for ET prior to PT in the atomistic models

For Systems 1a-1c and 2a-2c, we now discuss the auxiliary restraining potential introduced to restrict equilibrium sampling of the system to the ET channel in the sequential mechanism. This potential is given by

$$U_{\text{SET}}(\theta_p) = \begin{cases} a_{\text{SET}} (\theta_p - b_{\text{SET}})^2, & \theta_p < b_{\text{SET}} \\ 0, & \text{otherwise.} \end{cases} \quad (\text{S.68})$$

The coefficients a_{SET} a.u. and b_{SET} are chosen to correctly restrict the system to the ET channel and are provided in Table S6.

Table S6: Parameters for the auxiliary restraining potential in Eq. S.68.^a

System	a_{SET}	b_{SET}
1a	1000	0.25
1b	1000	0.21
1c	1000	0.20
2a	1000	0.15
2b	1000	0.08
2c	1000	0.08

^a a_{SET} is given in units of kcal/mol Å⁻². b_{SET} is given in units of Å.

4.3 Auxiliary restraining potential for concerted PCET in the system-bath models

For Systems 3a-3e, 4a-4e, and 5a-5e, we now discuss the auxiliary restraining potential introduced to restrict equilibrium sampling of the system to the concerted channel in the system-bath model. This potential is given by

$$U_{\text{aux}}(\bar{q}_{\text{p}}, \theta_{\text{e}}) = \begin{cases} a_{\text{aux}} [\bar{q}_{\text{p}} - q_{+}(\theta_{\text{e}})]^2, & \bar{q}_{\text{p}} > q_{+}(\theta_{\text{e}}) \\ a_{\text{aux}} [\bar{q}_{\text{p}} - q_{-}(\theta_{\text{e}})]^2, & \bar{q}_{\text{p}} < q_{-}(\theta_{\text{e}}) \\ 0, & \text{otherwise} \end{cases} \quad (\text{S.69})$$

where

$$q_{+}(\theta_{\text{e}}) = b_{\text{aux}}\theta_{\text{e}} + c_{\text{aux}} \quad (\text{S.70})$$

and

$$q_{-}(\theta_{\text{e}}) = b_{\text{aux}}\theta_{\text{e}} - c_{\text{aux}}. \quad (\text{S.71})$$

The coefficients a_{aux} , b_{aux} , and c_{aux} (Table S7) are chosen to restrict the system to the concerted channel.

Table S7: Parameters for the auxiliary restraining potential in Eq. S.69^a.

System	a_{aux}	b_{aux}	c_{aux}
3a	1.0	0.57	0.32
3b	1.0	0.56	0.32
3c	1.0	0.56	0.32
3d	1.0	0.55	0.33
3e	1.0	0.55	0.33
4a	1.0	0.55	0.32
4b	1.0	0.55	0.34
4c	1.0	0.56	0.35
4d	1.0	0.57	0.36
4e	1.0	0.58	0.38
5a	1.0	0.57	0.33
5b	1.0	0.56	0.33
5c	1.0	0.55	0.33
5d	1.0	0.55	0.33
5e	1.0	0.55	0.33

^a a_{aux} is given in units of a.u. $\times 10^{-2}$; all other parameters are given in atomic units.

4.4 Auxiliary restraining potential for ET prior to PT in the system-bath models

For Systems 3a-3e, 4a-4e, and 5a-5e, we now discuss the auxiliary restraining potential introduced to restrict equilibrium sampling of the system to the ET channel in the sequential mechanism. This potential is given by

$$U_{\text{SET}}(\bar{q}_{\text{p}}) = \begin{cases} a_{\text{SET}} (\bar{q}_{\text{p}} - b_{\text{SET}})^2, & \bar{q}_{\text{p}} < b_{\text{SET}} \\ 0, & \text{otherwise.} \end{cases} \quad (\text{S.72})$$

The coefficients a_{SET} a.u. and b_{SET} are chosen to correctly restrict the system to the ET channel and are provided in Table S8.

Table S8: Parameters for the auxiliary restraining potential in Eq. S.72.

System	a_{SET}	b_{SET}
1a	1.0	0.29
1b	1.0	0.29
1c	1.0	0.29
1d	1.0	0.29
1e	1.0	0.29
2a	1.0	0.20
2b	1.0	0.20
2c	1.0	0.20
2d	1.0	0.23
2e	1.0	0.26
3a	1.0	0.30
3b	1.0	0.30
3c	1.0	0.30
3d	1.0	0.30
3e	1.0	0.30

^a a_{SET} is given in units of a.u. $\times 10^{-2}$. b_{SET} is given in units of a.u.

References

- (S1) Craig, I. R.; Manolopoulos, D. E. *J. Chem. Phys.* **2004**, *121*, 3368–3373.
- (S2) Miller, T. F., III *J. Chem. Phys.* **2008**, *129*, 194502.
- (S3) Kretchmer, J. S.; Miller, T. F., III *J. Chem. Phys.* **2013**, *138*, 134109.
- (S4) Steele, R. P.; Zwickl, J.; Shushkov, P.; Tully, J. C. *J. Chem. Phys.* **2011**, *134*, 074112.
- (S5) Wigner, E. *Phys. Chem. Abt. B* **1932**, *19*, 203–216.
- (S6) Eyring, H. *J. Chem. Phys.* **1935**, *3*, 107–115.
- (S7) Keck, J. C. *J. Chem. Phys.* **1960**, *32*, 1035–1050.
- (S8) Craig, I. R.; Manolopoulos, D. E. *J. Chem. Phys.* **2005**, *122*, 084106.
- (S9) Craig, I. R.; Manolopoulos, D. E. *J. Chem. Phys.* **2005**, *123*, 34102.
- (S10) Miller, W. H. *J. Chem. Phys.* **1973**, *58*, 1664–1667.
- (S11) Chandler, D. *J. Chem. Phys.* **1978**, *68*, 2959–2970.
- (S12) Bennet, C. H. In *Algorithms for Chemical Computations*; Christofferson, R. E., Ed.; American Chemical Society: Washington, DC, 1977; p 63.
- (S13) Collepardo-Guevara, R.; Craig, I. R.; Manolopoulos, D. E. *J. Chem. Phys.* **2008**, *128*, 144502.
- (S14) Menzeleev, A. R.; Ananth, N.; Miller, T. F., III *J. Chem. Phys.* **2011**, *135*, 074106.
- (S15) Carter, E. A.; Ciccotti, G.; Hynes, J. T.; Kapral, R. *Chem. Phys. Lett.* **1989**, *156*, 472–477.
- (S16) Schenter, G. K.; Garrett, B. C.; Truhlar, D. G. *J. Chem. Phys.* **2003**, *119*, 5828–5833.
- (S17) Watney, J. B.; Soudackov, A. V.; Wong, K. F.; Hammes-Schiffer, S. *Chem. Phys. Lett.* **2006**, *25*, 268–271.

- (S18) Parrinello, M.; Rahman, A. *J. Chem. Phys.* **1984**, *80*, 860–867.
- (S19) Roth, J. P.; Lovell, S.; Mayer, J. M. *J. Am. Chem. Soc.* **2000**, *122*, 5486–5498.
- (S20) Wang, J.; Wolf, R. M.; Caldwell, J. W.; Kollman, P. A.; Case, D. A. *J. Comp. Chem.* **2004**, *25*, 1157–1174.
- (S21) Guardia, E.; Pinzon, R.; Casulleras, J.; Orozco, M.; Luque, F. J. *Mol. Simulat.* **2001**, *26*, 287–306.
- (S22) Breneman, C. M.; Wiberg, K. B. *J. Comp. Chem.* **1990**, *11*, 361–373.
- (S23) Frisch, M. J.; Trucks, G. W.; Schlegel, H. B.; Scuseria, G. E.; Robb, M. A.; Cheeseman, J. R.; Scalmani, G.; Barone, V.; Mennucci, B.; Petersson, G. A.; Nakatsuji, H.; Caricato, M.; Li, X.; Hratchian, H. P.; Izmaylov, A. F.; Bloino, J.; Zheng, G.; Sonnenberg, J. L.; Hada, M.; Ehara, M.; Toyota, K.; Fukuda, R.; Hasegawa, J.; Ishida, M.; Nakajima, T.; Honda, Y.; Kitao, O.; Nakai, H.; Vreven, T.; Montgomery, J. A., Jr.; Peralta, J. E.; Ogliaro, F.; Bearpark, M.; Heyd, J. J.; Brothers, E.; Kudin, K. N.; Staroverov, V. N.; Kobayashi, R.; Normand, J.; Raghavachari, K.; Rendell, A.; Burant, J. C.; Iyengar, S. S.; Tomasi, J.; Cossi, M.; Rega, N.; Millam, J. M.; Klene, M.; Knox, J. E.; Cross, J. B.; Bakken, V.; Adamo, C.; Jaramillo, J.; Gomperts, R.; Stratmann, R. E.; Yazyev, O.; Austin, A. J.; Cammi, R.; Pomelli, C.; Ochterski, J. W.; Martin, R. L.; Morokuma, K.; Zakrzewski, V. G.; Voth, G. A.; Salvador, P.; Dannenberg, J. J.; Dapprich, S.; Daniels, A. D.; Farkas, .; Foresman, J. B.; Ortiz, J. V.; Cioslowski, J.; Fox, D. J. *Gaussian?09 Revision D.01*. Gaussian Inc. Wallingford CT 2009.
- (S24) Azzouz, H.; Borgis, D. *J. Chem. Phys.* **1993**, *98*, 7361–7375.
- (S25) Warshel, A. *Computer modeling of chemical reactions in enzymes and solutions*; John Wiley: New York, 1991.

- (S26) Iordanova, N.; Decornez, H.; Hammes-Schiffer, S. *J. Am. Chem. Soc.* **2001**, *123*, 3723–3733.
- (S27) Kuharski, R. A.; Bader, J. S.; Chandler, D.; Sprik, M.; Klein, M. L.; Impey, R. W. *J. Chem. Phys.* **1988**, *89*, 3248–3257.
- (S28) Coker, D. F.; Berne, B. J.; Thirumalai, D. *J. Chem. Phys.* **1987**, *89*, 5689–5702.
- (S29) Manner, V. W.; DiPasquale, A. G.; Mayer, J. M. *J. Am. Chem. Soc.* **2008**, *130*, 7210–7211.
- (S30) Manner, V. W.; Mayer, J. M. *J. Am. Chem. Soc.* **2009**, *131*, 9874–9875.
- (S31) Warren, J. J.; Menzeleev, A. R.; Kretchmer, J. S.; Miller, T. F., III; Gray, H. B.; Mayer, J. M. *J. Phys. Chem. Lett.* **2013**, 519–523.
- (S32) Caldeira, A. O.; Leggett, A. J. *Annals of Physics* **1983**, *149*, 374–456.
- (S33) Leggett, A. J.; Chakravarty, S.; Dorsey, A. T.; Fisher, M. P. A.; Garg, A.; Zwerger, W. *Rev. Mod. Phys.* **1987**, *59*, 1–85.
- (S34) Topaler, M.; Makri, N. *J. Chem. Phys.* **1994**, *101*, 7500–7519.
- (S35) Smith, W.; Forester, T. R. *J. Mol. Graph.* **1996**, *14*, 136–141.
- (S36) Verlet, L. *Phys. Rev.* **1967**, *159*, 98–103.
- (S37) Habershon, S.; Manolopoulos, D. E.; Markland, T. E.; Miller, T. F., III *Annu. Rev. Phys. Chem.* **2013**, *64*, 387–413.
- (S38) Brooks, C. L.; Pettitt, B. M.; Karplus, M. *J. Chem. Phys.* **1985**, *83*, 5897–5908.
- (S39) Newton, M. D.; Sutin, N. *Ann. Rev. Phys. Chem.* **1984**, *35*, 437–480.
- (S40) Smith, W.; Forester, T. R. *Prog. Inorg. Chem.* **1983**, *30*, 441–498.
- (S41) Raedt, B. D.; Sprik, M.; Klein, M. L. *J. Chem. Phys.* **1984**, *80*, 5719–5724.

- (S42) Andersen, H. C. *J. Comput. Phys.* **1983**, *52*, 24–34.
- (S43) King, G.; Warshel, A. *J. Chem. Phys.* **1990**, *93*, 8682–8692.
- (S44) Soudackov, A.; Hammes-Schiffer, S. *J. Chem. Phys.* **2000**, *113*, 2385–2396.
- (S45) Hammes-Schiffer, S.; Stuchebrukhov, A. A. *Chem. Rev.* **2010**, *110*, 6939–6960.
- (S46) Boekelheide, N.; Salomón-Ferrer, R.; Miller, T. F., III *Proc. Natl. Acad. Sci.* **2011**, *108*, 16159–16163.
- (S47) Bolhuis, P. G.; Chandler, D.; Dellago, C.; Geissler, P. L. *Annu. Rev. Phys. Chem.* **2002**, *53*, 291–318.
- (S48) Hummer, G. *J. Chem. Phys.* **2004**, *120*, 516–523.
- (S49) Vanden-Eijnden, E. W. *J. Stat. Phys.* **2006**, *123*, 503–523.